SUPPLEMENTARY INFORMATION

doi:10.1038/nature11265

I. NANOTUBE QUANTUM DOTS

The nanotubes are grown by chemical vapor deposition from a CH_4 feedstock gas [1] on a Si/SiO_2 substrate coated with Fe/Mo catalyst nanoparticles [2, 3], usually producing nanotubes with diameters of about 2 nm. Individual nanotubes are contacted by metallic leads, thereby forming quantum dots, and controlled by three gates: a back gate that changes the number of electrons in the nanotube and two side gates (SG_1 and SG_2), located closer to either the source or the drain electrodes. Applying the side gate voltage V_{SG} modifies the relative strength of tunneling from the nanotube to the source and the drain. It turns out that it is sufficient to bias only one of the side gates, as done in this paper.

Figure 1B of the main text shows a typical plot of the nanotube conductance *vs.* gate voltage (the "Coulomb blockade pattern"). A group of 4 peaks of similar height is visible on the left, corresponding to filling a 4-electron "shell" [4, 5]. The peaks in the group are separated from neighboring groups by wider Coulomb blockade valleys Y and Z, in which an integer number of shells is completely filled. In this regime, the electron transport through the nanotube is determined by the co-tunneling processes (Figure S1), which are almost energy-independent on the energy scales smaller than the charging energy or the level spacing (*i.e.* meV's). In this case, the nanotube essentially behaves as a lumped tunnel junction. As discussed below and in the main text, this allows us to *in situ* characterize the suppression of tunneling conductance due to the resistive leads (Figures 1C-D of the main text).

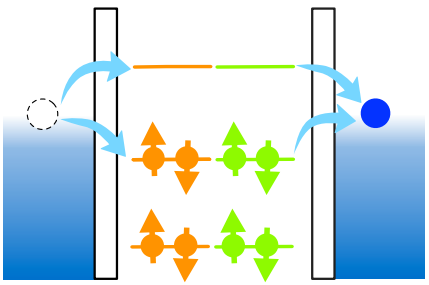

Figure S 1: Schematic: an energy diagram of a Coulomb blockade valley, in which an integer number of 4-electron shells is filled (like valleys Y or Z in Figure 1 of the main text). Cotunneling is the dominant process that contributes to the electron transport through the quantum dot: an electron from the source can virtually occupy a high energy orbital in the dot and then tunnel out; alternatively an electron can tunnel out of a filled orbital, followed by an electron from the lead filling the empty state.

II. DISSIPATIVE ENVIRONMENT

The strength of dissipation in the resistive leads is characterized by $r = e^2R/h$, where R is the total resistance of the two leads. The leads are made from a Cr/Au (10nm/1nm) film with a resistivity of 75 $\Omega/\square$, and their total room temperature resistance is estimated at ~ 6.5 kΩ for the sample shown in Figure 1 of the main text, and ~ 17 kΩ for the sample shown in Figures 2-3. These numbers yield $r \sim 0.25$ for the first sample, and $r \sim 0.65$ for the second sample. However the film resistivity increases by at least 10% at low temperature, making these estimates consistent with $r = 0.3$ we extract in Figure 1D for the first sample, and $r = 0.75$ extracted for the second sample (see the next paragraph).

According to the theory of tunneling with dissipation (also referred to as "environmental Coulomb blockade" [6–12]), in order to determine the dissipation strength, one has to consider the impedance of the whole circuit at frequencies corresponding to temperature or bias (*i.e.* $\hbar\omega \sim k_BT$ or eV). In our case, this frequency range extends from ~ 1 GHz up to ~ 100 GHz. The lithographically made resistive leads connect the nanotubes to much larger pads (hundreds of microns on a side), whose capacitance short-circuits the high frequency fluctuations. Therefore, only the on-chip resistance of the leads contributes to dissipation. We also estimate that the distributed capacitance of the resistive leads can be neglected in this frequency range, so that the leads behave as simple frequency - independent resistors.

We choose to demonstrate two different aspects of the observed behavior in two samples. The sample shown in Figure 1 has the smaller dissipation strength of $r = 0.3$, resulting in the striking cusp $G \propto |V|^{2r}$ in Figure 1C. In Figures 2-4, we extract the peak width proportional to $T^{r/(r+1)}$. The relatively large dissipation strength of this sample is required to distinguish this non-trivial exponent a from the dependence T^r predicted by the lower-order theoretical considerations.

Tunneling current $I(V,T)$ through a single tunneling bar-

rier in the case of Ohmic dissipation was obtained in Ref. [12]:

$$I(V,T) \propto VT^{2r}\left|\frac{\Gamma[r+1+i\frac{eV}{2\pi k_B T}]}{\Gamma[1+i\frac{eV}{2\pi k_B T}]}\right|^2 \qquad (1)$$

We numerically differentiate this expression with respect to V to fit the data in Figure 1d of the main text.

III. ESTIMATES OF THE EXPONENTS

Asymmetric peak height. Figure 3A shows the temperature dependence of the peak height for various degrees of asymmetry between the tunneling rate from the level to the source and the drain electrodes, Γ_S and Γ_D. Depending on the asymmetry, the peak conductance exhibits a range of cross-over behaviors. For peaks with low degree of asymmetry (such that $|\Gamma_S - \Gamma_D| \sim k_B T \ll |\Gamma_S + \Gamma_D|$, top curves), the proper temperature scaling of conductance is not yet fully developed, so care must be taken to avoid extracting an incorrect exponent. Hence we study the conductance scaling of the most asymmetric peak of Figure 3A (reproduced here in Figure S2), which demonstrates a fully developed power-law behavior in the accessible temperature range. A linear curve is fitted to the data on a log-log scale in the temperature range of 0.08 K $< T <$ 1.2 K. The extracted slope of 1.47 $\pm$ 0.04 corresponds to the value of $r = 0.74 \pm 0.02$.

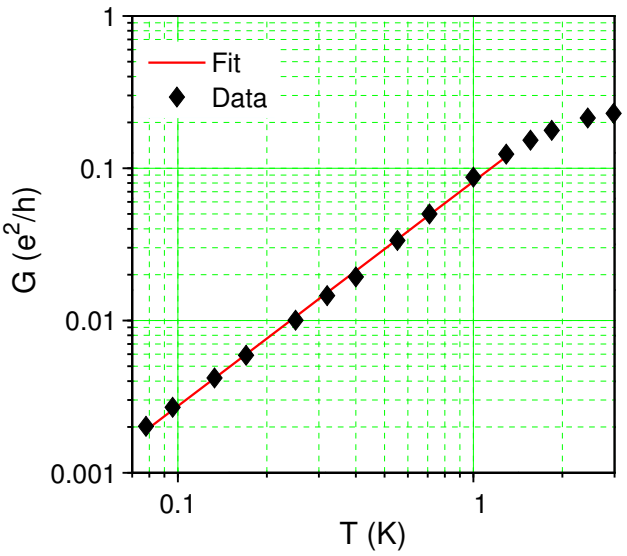

Figure S2: Conductance of an asymmetrically coupled peak *vs.* temperature (same data as the lowest curve in Figure 3A), and the power-law fit. The uncertainty in the data points is about the symbol size.

Symmetric resonance width. The full-width at half-maximum (FWHM) of the symmetric peak (Figure 2A) is plotted in Figure S3. The fit shown in red yields an exponent of 0.43 $\pm$ 0.01, surprisingly close to the expected value of $r/(r+1) \approx 0.43$. (In order to avoid over-estimating the exponent, the $T > 1$ K data points are not included in the fit. This higher temperature range corresponds to the transition to the sequential tunneling regime $k_B T \gtrsim \Gamma$, in which case the peak width becomes proportional to T.)

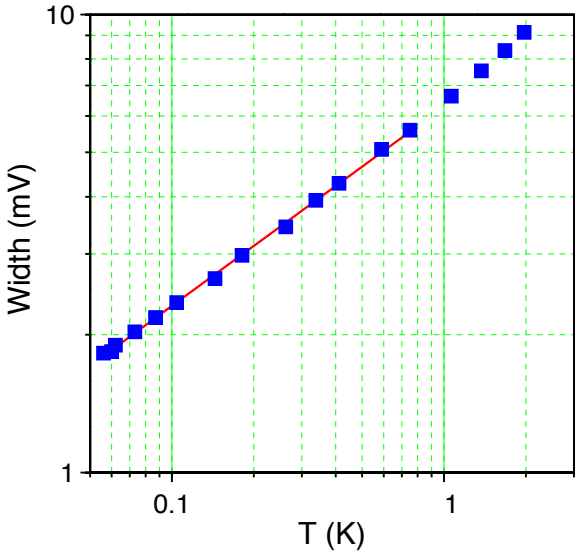

Figure S3: Full-width at half-maximum extracted from the symmetric peak in Figure 2B. In order to exclude the contribution from the sequential tunneling regime $k_B T \gtrsim \Gamma$, only the data points measured at $T < 1$ K are used for the fit shown in red (see text). The vertical axis has to be multiplied by the experimentally determined "gate efficiency factor" of ≈ 0.2, which converts ΔV_{gate} units to the actual energy of the resonant level (see e.g. Ref [13]).

Before proceeding to the theoretical model, we note that our observations cannot be explained by the conventional Lorentzian expression for the resonance conductance between non-interacting leads [14]. First, the line shape of the resonances is not Lorentzian. Second, even if one tries to describe the symmetric case by a Lorentzian with temperature-dependent tunneling rates $\Gamma_{S,D}(T)$, in the asymmetric case the same expression would also yield a peak with a temperature-independent height and a vanishing width, in marked contrast with our measurements in Fig. 2c.

IV. MODEL

We model our experimental situation by a spinless level coupled to two conducting leads in the presence of an Ohmic dissipative environment (Figure S4). As we show in the following, the electromagnetic modes of the environment mediate interactions between the electrons in the leads, resulting in a Luttinger liquid-like behavior. We start with a system Hamiltonian given by

$$H = H_{\rm Dot} + H_{\rm Leads} + H_{\rm T} + H_{\rm Env} \tag{2}$$

and describe the individual terms in this section. $H_{\rm Dot} = \epsilon_{\rm d} d^\dagger d$ is the Hamiltonian of the dot with the energy level $\epsilon_{\rm d}$ and the electron creation operator $d^\dagger$. $H_{\rm Leads} = \sum_{\alpha={\rm S,D}} \sum_k \epsilon_k c^\dagger_{k\alpha} c_{k\alpha}$ represents the electrons in the source (S) and drain (D) leads.

$H_{\rm T}$ describes the tunneling between the dot and the leads:

$$H_{\rm T} = V_S \sum_k (c^\dagger_{kS} e^{-i\varphi_S} d +) + V_D \sum_k (c^\dagger_{kD} e^{i\varphi_D} d + {\rm h.c.}), \tag{3}$$

where the operators $\varphi_{S/D}$ represent the phase fluctuations of the tunneling amplitude between the dot and the S/D lead. These phase operators are canonically conjugate to the operators $Q_{S/D}$ corresponding to charge fluctuations on the S/D junctions. This is a standard way to treat macroscopic quantum tunneling in the presence of a dissipative environment [8], which is valid for electrons propagating much slower than the electromagnetic field [15].

It is useful to transform to variables related to the total charge on the dot. To that end, we introduce [8] two new phase operators, φ and ψ, related to the phases $\varphi_{S/D}$ by

$$\begin{aligned} \varphi_S &= \kappa_S \varphi + \psi \\ \varphi_D &= \kappa_D \varphi - \psi \,, \end{aligned} \tag{4}$$

where $\kappa_{S/D} = C_{D/S}/(C_S + C_D)$ in terms of the capcitances of the two dots, $C_{S/D}$. ψ is the variable conjugate to the fluctuations of charge on the dot $Q_c = Q_S - Q_D$ and so couples to voltage fluctuations on the gate which controls the energy of the dot's level. Likewise, φ is the variable conjugate to $Q = (C_S Q_D + C_D Q_S)/(C_D + C_S)$. Assuming $C_S = C_D$, we have $\varphi_S = \varphi/2 + \psi$ and $\varphi_D = \varphi/2 - \psi$.

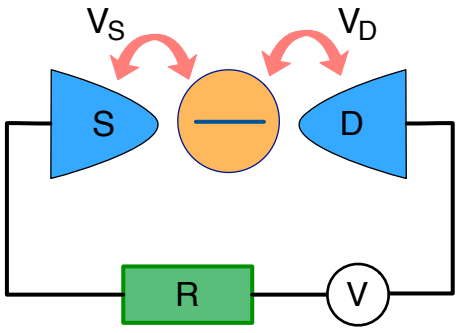

Figure S 4: Schematic: a spinless quantum dot is coupled to two conducting leads with tunneling amplitudes V_S and V_D. The dot-leads system is attached to a voltage source V via R, the sum of the lead resistances.

The gate voltage fluctuations can be disregarded in our experiment because the capacitance of the gate is negligible, $C_g \ll C_{S/D}$. (The opposite limit of a noisy gate coupled to a resonant level was considered in Ref. 16.) In fact, for our purposes, the coupling of the fluctuations of the total charge on the dot to the environment can be neglected. Thus, only the *relative* phase difference between the two leads remains [8, 17], and the tunneling Hamiltonian becomes

$$H_{\rm T} = V_S \sum_k (c^\dagger_{kS} e^{-i\frac{\varphi}{2}} d + {\rm h.c.}) + V_D \sum_k (c^\dagger_{kD} e^{i\frac{\varphi}{2}} d + {\rm h.c.}). \tag{5}$$

The last part of Eq. (2) is the Hamiltonian of the environment, $H_{\rm Env}$ [8, 18, 19]. The environmental modes are represented by harmonic oscillators described by inductances and capcitances such that their frequencies are given by $\omega_n = 1/\sqrt{L_n C_n}$. These oscillators are then bilinearly coupled to the phase operator φ through the oscillator phase:

$$H_{\rm Env} = \frac{Q^2}{2C} + \sum_{n=1}^{N} \left[\frac{q_n^2}{2C_n} + \left(\frac{\hbar}{e}\right)^2 \frac{1}{2L_n} (\varphi - \varphi_n)^2 \right]. \tag{6}$$

V. MAPPING TO LUTTINGER LIQUIDS

In this section, we demonstrate the mapping of our model to that of a resonant level contacted by two Luttinger liquids. In carrying out this mapping, we follow closely previous work on tunneling through a single barrier with an environment [20, 21] and the Kondo effect in the presence of resistive leads [17].

The two metallic leads in our case can be reduced to two semi-infinite one-dimensional free fermionic baths, which are non-chiral [22]. By unfolding them, one can obtain two chiral fields [22], which both couple to the dot at $x = 0$. We bosonize the fermionic fields in the standard way [22, 23] $c_{S/D}(x) = \frac{1}{\sqrt{2\pi a}} F_{S/D} \exp[i\phi_{S/D}(x)]$. Here, $F_{S/D}$ is the Klein factor, $\phi_{S/D}$ is the bosonic field, and a is the short time cutoff. Defining the flavor field ϕ_f and charge field ϕ_c by

$$\phi_f \equiv \frac{\phi_S - \phi_D}{\sqrt{2}}, \qquad \phi_c \equiv \frac{\phi_S + \phi_D}{\sqrt{2}}, \tag{7}$$

we rewrite the Hamiltonian of the leads as

$$H_{\rm Leads} = \frac{v_F}{4\pi} \int_{-\infty}^{\infty} dx \left[(\partial_x \phi_c)^2 + [(\partial_x \phi_f)^2 \right]. \tag{8}$$

The tunneling Hamiltonian then becomes

$$H_{\rm T} = V_S \left(\frac{1}{\sqrt{2\pi a}} F_S \exp\left[-i \frac{\phi_c(0) + \phi_f(0)}{\sqrt{2}} \right] e^{-i\frac{\varphi}{2}} d + \text{h.c.} \right) + V_D \left(\frac{1}{\sqrt{2\pi a}} F_D \exp\left[-i \frac{\phi_c(0) - \phi_f(0)}{\sqrt{2}} \right] e^{i\frac{\varphi}{2}} d + \text{h.c.} \right) . \quad (9)$$

Note a key feature of $H_{\rm T}$: the fields φ and $\phi_f(0)$ enter in the same way. Thus we wish to combine these two fields, a process which will lead to effectively interacting leads as in a Luttinger liquid.

To carry out such a combination, since the tunneling only acts at $x = 0$, it is convenient to perform a partial trace in the partition function and integrate out fluctuations in $\phi_{c/f}(x)$ for all x away from $x = 0$ [24]. For an Ohmic environment, one can also integrate out the harmonic modes [17, 19, 20]. Then, the effective action for the leads and the environment becomes

$$S^{\rm eff}_{\rm Leads+Env} = \frac{1}{\beta} \sum_n |\omega_n| \left(|\phi_c(\omega_n)|^2 + |\phi_f(\omega_n)|^2 + \frac{R_Q}{2R} |\varphi(\omega_n)|^2 \right) , \quad (10)$$

where $R_Q = h/e^2$, R is the total resistance of the leads, and $\omega_n = 2\pi n/\beta$ is the Matsubara frequency. In this discrete representation, it is straightforward to combine the phase operator φ and the flavor field ϕ_f; in order to maintain canonical commutation relations while doing so, we use the transformation

$$\phi'_f \equiv \sqrt{g_f} \left(\phi_f + \frac{1}{\sqrt{2}} \varphi \right) , \qquad \varphi' \equiv \sqrt{g_f} \left(\sqrt{\frac{R}{R_Q}} \phi_f - \sqrt{\frac{R_Q}{R}} \frac{1}{\sqrt{2}} \varphi \right) , \quad (11)$$

where $g_f \equiv 1/(1 + R/R_Q) < 1$. Now, the effective action for the leads and environment (excluding tunneling) becomes

$$S^{\rm eff}_{\rm Leads+Env} = \frac{1}{\beta} \sum_n |\omega_n| \left(|\phi_c(\omega_n)|^2 + |\phi'_f(\omega_n)|^2 + |\varphi'(\omega_n)|^2 \right) , \quad (12)$$

while the Lagrangian for the tunneling part reads

$$L_{\rm T} = -V_S \left(\frac{F_S}{\sqrt{2\pi a}} e^{-i\frac{1}{\sqrt{2g_c}}\phi_c(\tau)} e^{-i\frac{1}{\sqrt{2g_f}}\phi'_f(\tau)} d + \text{c.c.} \right) - V_D \left(\frac{F_D}{\sqrt{2\pi a}} e^{-i\frac{1}{\sqrt{2g_c}}\phi_c(\tau)} e^{i\frac{1}{\sqrt{2g_f}}\phi'_f(\tau)} d + \text{c.c.} \right) . \quad (13)$$

(Here, we have formally introduced the parameter $g_c = 1$ to describe the noninteracting field ϕ_c.) Indeed, we see that the phase φ has been absorbed into the new flavor field ϕ'_f at the expense of a modified interaction parameter g_f, while the new phase fluctuation φ' decouples from the system. In what follows, we will drop the prime from the operator ϕ'_f.

It turns out that one obtains a very similar effective action by starting from a model with resonant tunneling between Luttinger liquids [24, 25]. The two models are equivalent if the interaction parameters g_c and g_f in our model are made equal to the single interaction parameter g of Ref. 24. Similar mappings were obtained for a spinful model in the absence of charge fluctuations (Kondo regime) in Ref. 17 and for a dissipative dot coupled to a single chiral Luttinger liquid in Ref. 21.

As discussed in the main text, the $r = 0$ case ($g_f = 1$) reduces to a resonant level without dissipation, while the $r = 1$ case ($g_f = 1/2$) can be mapped onto the two-channel Kondo model. To understand the relation between our model and the two-channel Kondo model, we apply a unitary transformation [26, 27], $U = \exp[i(d^\dagger d - 1/2)\phi_c(0)/\sqrt{2}]$, to eliminate the ϕ_c field in the tunneling Lagrangian, Eq. (13). At the same time, an extra electrostatic Coulomb interaction between the leads and the dot is generated. Introducing in addition a bare electrostatic Coulomb interaction (U_b), we have

$$H_C = \frac{\sqrt{2}}{\pi} (U_b - 1)(d^\dagger d - 1/2) \partial_x \phi_c(x = 0) . \quad (14)$$

For the special value $g_f = 1/2$, we can refermionize the problem by defining $\psi_{c,f} = e^{i\phi_{c,f}}/\sqrt{2\pi a}$. Then, at $V_S = V_D$ (and $r = 1$), our model is mapped onto the two-channel Kondo model [26–29], which shows non-Fermi-liquid behavior [30]. At the Toulouse point ($U_b = 1$ so that $H_C = 0$), the model reduces to a Majorana resonant level model [26, 30]. Finally, for r close to 1 (*i.e.* in our case), one can similarly map our system onto a two-channel Kondo model with (interacting) Luttinger liquid leads [28, 29]. The effective interaction parameter g_σ in this case is determined by the residual $1 - r$.

VI. QUANTUM PHASE TRANSITION AND SCALING RELATIONS

Having established the relation between our problem and Luttinger liquid physics, we can draw on the very extensive theoretical work concerning resonant tunneling in a Luttinger liquid [24, 27, 31–35] to reach conclusions about the scaling and phase transitions implied by our model. To understand how the interacting environment affects the low temperature physics, it is convenient to rewrite the model, following Refs. 24 and 36, in the "Coulomb-gas" representation, which can be accomplished by expanding the partition function in powers of V_S and V_D. After integrating out $\phi_f(\tau)$ and $\phi_c(\tau)$ in each term, one obtains a classical one-dimensional statistical mechanics problem with the partition function

$$
\begin{aligned}
Z &= \sum_{\sigma=\pm}\sum_{n}\sum_{\{q_i=\pm\}} V_S^{\sum_i (1+q_i p_i)/2} V_D^{\sum_i (1-q_i p_i)/2} \\
&\quad \times \int_0^{\beta} d\tau_{2n} \int_0^{\tau_{2n}} d\tau_{2n-1} \ldots\ldots \int_0^{\tau_2} d\tau_1 \exp\Big\{\sum_{i<j} V_{ij}\Big\} \exp\left\{\epsilon_d\Big[\beta\frac{1-\sigma}{2} + \sigma \sum_{1\le i\le 2n} p_i\tau_i\Big]\right\}, \\
V_{ij} &= \frac{1}{2g_f}\left[q_iq_j + K_1 p_i p_j + K_2(p_iq_j + p_jq_i)\right] \ln\left(\frac{\tau_i-\tau_j}{\tau_c}\right) . \qquad (15)
\end{aligned}
$$

We consider the on-resonance case, $\epsilon_d = 0$, so that the last term in the partition function is equal to 1. There are two types of charges in this 1D problem [24]: q_i charge and p_i charge, both of which can be ± 1. The total system is charge neutral, $\sum_i q_i = \sum_i p_i = 0$. Physically, the q_i charge corresponds to a tunneling event between the dot and the leads ($+1$: to the right (D); -1: to the left (S)). The p_i charge corresponds to hopping onto $(+1)$ or off (-1) the dot.

Following the method developed for resonant tunneling between Luttinger liquids in Ref. 24, one obtains the renormalization group (RG) equations and the phase diagram. The sign of the p_i charge must alternate in time, while the q_i charge can have any ordering satisfying the charge neutrality constraint. Therefore, the interaction between the q_i charges does not vary in the RG flow, while the interaction strength between p_i charges, K_1, does renormalize. The bare K_1 (initial value in RG flow) is $K_1^{\rm bare} = g_f/g_c$; in fact, by taking into account the coupling of the fluctuations of the total dot charge to the environment—an effect neglected here—one can show that $K_1^{\rm bare} = 1$ [37]. The bare value of K_2 is zero, but it will be generated in the RG flow. These are the same conditions as in resonant tunneling between two Luttinger liquids [24]. Hence, our model is mapped onto the model of resonant tunneling between Luttinger liquids, with the RG equations for the interaction strengths and tunneling couplings as in Ref. 24.

The resulting schematic RG flow diagram in the V_S-V_D plane, valid for $r < 1$ and on-resonance, is shown in Figure S5. A remarkable feature of this RG flow diagram is that a second order quantum phase transition can be realized by tuning the tunneling matrix element across the symmetric coupling line, $V_S = V_D$. Indeed, this critical value separates the flows terminating in the stable fixed points denoted as $(0,1)$ and $(1,0)$ in Figure S5. These two phases correspond to the dot merging with the D lead, while the S lead decouples, or *vice versa*. The unstable fixed point denoted as $(1,1)$ is reached starting exactly at $V_S = V_D$; it corresponds to a *homogeneous* Luttinger liquid which therefore has conductance $G = e^2/h$

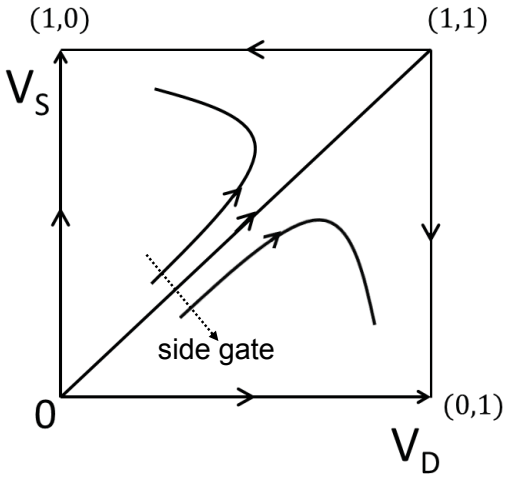

Figure S 5: Schematic representation of the renormalization group flow for the two tunneling amplitudes, V_S and V_D [24]. The diagonal corresponds to the symmetric coupling case, and flows into the strongly coupled quantum critical point at (1,1) which corresponds to a single homogeneous Luttinger liquid. Point (1,0) describes the strong coupling point for V_S, while $V_D = 0$; similarly, point (0,1) describes the strong coupling point for V_D, while $V_S = 0$.

[24, 31].

The proximity to the strongly coupled point $(1, 1)$ determines the quantum critical behavior and the critical exponents observed in the experiment. By analyzing the universal scaling function [24], the width of the resonant peak is found to scale to zero as $\Gamma \propto T^{1-g_f} = T^{r/(1+r)}$. For the case of asymmetric tunneling $V_S \neq V_D$, either V_S or V_D flows to zero so that the height of the resonant peak scales as $G \propto T^{2(1/g_f-1)=} = T^{2r}$ [24], while the width of the resonance saturates [27, 33, 34].

These power-law dependencies are typical for the critical behavior near a second-order phase transition. We would like to stress that this behavior qualitatively differs from the Kosterlitz-Thouless (KT) type of transition, commonly encountered in quantum impurity models [38]. For example, several recent theoretical works predict KT transitions in quantum dots coupled to a single interactive lead [39–43]. There, the QPT occurs when the dissipation exceeds a certain critical value. In our case, the crucial ingredient that enables the QPT is the symmetric coupling to the two leads, which allows for their competition, while the dissipation strength can be relatively weak (but greater than zero).

[1] J. Kong, H. T. Soh, A. M. Cassell, C. F. Quate, and H. Dai, Nature **395**, 878 (1998).

[2] Y. Li, J. Liu, Y. Wang, and Z. Wang, Chem. Mat. **13**, 1008 (2001).

[3] L. An, J. M. Owens, L. E. McNeil, and J. Liu, J. Am. Chem. Soc. **124**, 13688 (2002).

[4] W. Liang, M. W. Bockrath, and H. Park, Phys. Rev. Lett. **88**, 126801 (2002).

[5] M. Buitelaar, A. Bachtold, T. Nussbaumer, M. Iqbal, and C. Schonenberger, Phys. Rev. Lett. **88**, 156801 (2002).

[6] P. Delsing, K. K. Likharev, L. S. Kuzmin, and T. Claeson, Phys. Rev. Lett. **63**, 1180 (1989).

[7] A. N. Cleland, J. M. Schmidt, and J. Clarke, Phys. Rev. Lett. **64**, 1565 (1990).

[8] G.-L. Ingold and Yu.V. Nazarov, in *Single Charge Tunneling: Coulomb Blockade Phenomena in Nanostructures*, edited by H. Grabert and M. H. Devoret (Plenum, New York, 1992), pp. 21–107.

[9] K. Flensberg, S. Girvin, M. Jonson, and D. Penn, Physica Scripta **1992**, 189 (1992).

[10] J. P. Kauppinen and J. P. Pekola, Phys. Rev. Lett. **77**, 3889 (1996).

[11] P. Joyez, D. Esteve, and M. H. Devoret, Phys. Rev. Lett. **80**, 1956 (1998).

[12] W. Zheng, J. Friedman, D. Averin, S. Han, and J. Lukens, Solid State Communications **108**, 839 (1998).

[13] L. P. Kouwenhoven, C. M. Marcus, P. L. Mceuen, S. Tarucha, R. M. Westervelt, and N. S. Wingreen, in *Mesoscopic electron transport*, edited by L. L. Sohn, L. P. Kouwenhoven, and G. Schön (Kluwer, 1997), p. 105.

[14] M. A. Kastner, Physics Today **46**, 24 (1993).

[15] Yu.V. Nazarov and Y. M. Blanter, *Quantum Transport: Introduction to Nanoscience* (Cambridge University Press, Cambridge, 2009).

[16] H. Imam, V. Ponomarenko, and D. Averin, Phys. Rev. B **50**, 18288 (1994).

[17] S. Florens, P. Simon, S. Andergassen, and D. Feinberg, Phys. Rev. B **75**, 155321 (2007).

[18] A. O. Caldeira and A. J. Leggett, Phys. Rev. Lett. **46**, 211 (1981).

[19] A. J. Leggett, S. Chakravarty, A. T. Dorsey, M. P. A Fisher, A. Garg, W. Zwenger, *Rev. Mod. Phys.* **59**, 1 (1987).

[20] I. Safi and H. Saleur, Phys. Rev. Lett. **93**, 126602 (2004).

[21] K. Le Hur and M.-R. Li, Phys. Rev. B **72**, 073305 (2005).

[22] T. Giamarchi, *Quantum Physics in One Dimension* (Oxford University Press, New York, 2004).

[23] D. Senechal, in *Theoretical Methods for Strongly Correlated Electrons* (Springer-Verlag, New York, 2003).

[24] C. L. Kane and M. P. A. Fisher, Phys. Rev. B **46**, 15233 (1992).

[25] Forming linear combinations of the bosonic fields—such as we have done in showing the similarity of our problem to that of resonant tunneling in a Luttinger liquid—certainly leaves the thermodynamic properties and scaling of the coupling constants invariant. However, other properties, such as transport, may change. In fact, we can show that in the present case, transport properties are invariant as well (D.E. Liu, H. Zheng, H. T. Mebrahtu, G. Finkelstein, and H.U. Baranger, in preparation).

[26] V. J. Emery and S. Kivelson, Phys. Rev. B **46**, 10812 (1992).

[27] A. Komnik and A. O. Gogolin, Phys. Rev. Lett. **90**, 246403 (2003).

[28] M. Goldstein and R. Berkovits, Phys. Rev. B **82**, 161307 (2010).

[29] I. Affleck, private communication.

[30] A. O. Gogolin, A. A. Nersesyan, and A. M. Tsvelik, *Bosonization and Strongly Correlated Systems* (Cambridge University Press, 2004), pp. 384–408.

[31] S. Eggert and I. Affleck, Phys. Rev. B **46**, 10866 (1992).

[32] M. Sassetti, F. Napoli, and U. Weiss, Phys. Rev. B **52**, 11213 (1995).

[33] Yu. V. Nazarov and L. I. Glazman, Phys. Rev. Lett. **91**, 126804 (2003).

[34] D. G. Polyakov and I. V. Gornyi, Phys. Rev. B **68**, 035421 (2003).

[35] V. Meden, T. Enss, S. Andergassen, W. Metzner, and K. Schönhammer, Phys. Rev. B **71**, 041302 (2005).

[36] M. Goldstein and R. Berkovits, Phys. Rev. B **82**, 235315 (2010).

[37] D. E. Liu, H. Zheng, H. T. Mebrahtu, G. Finkelstein, and H. U. Baranger (2012), in preparation.

[38] M. Vojta, Philos. Mag. **86**, 1807 (2006).

[39] A. Furusaki and K. A. Matveev, Phys. Rev. Lett. **88**, 226404 (2002).

[40] K. Le Hur, Phys. Rev. Lett. **92**, 196804 (2004).

[41] L. Borda, G. Zaŕand, and D. Goldhaber-Gordon, arXiv.org (2006), available at http://arxiv.org/abs/cond-mat/0602019v2.

[42] C. H. Chung, M. T. Glossop, L. Fritz, M. Kirćan, K. Ingersent, M. Vojta, *Phys. Rev. B* **76** 235103 (2007).

[43] M. Cheng, M. T. Glossop, and K. Ingersent, Phys. Rev. B **80**, 165113 (2009).